2p2h final states in electron-Carbon scattering within the Spectral Function formalism

Noemi Rocco, A. Lovato, O. Benhar

INFN and Department of Physics, "Sapienza" Università di Roma

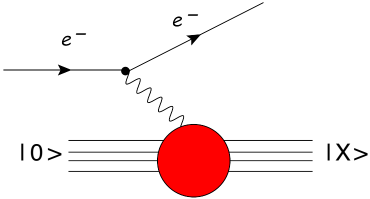

"Two-body current contributions in neutrino-nucleus scattering"
ESNT workshop 18-22 April 2016

Motivations

- Quantitative understanding of the nuclear response to neutrino interactions needed for the interpretation of neutrino oscillation signals

- The description of the neutrino-nucleus cross section involves non trivial additional difficulties, mostly owing to the broad distribution of the incoming neutrino energies

- Accurate theoretical models of electron- nucleus scattering provide a satisfactory description of the experimental data.

Motivations

- Quantitative understanding of the nuclear response to neutrino interactions needed for the interpretation of neutrino oscillation signals
- The description of the neutrino-nucleus cross section involves non trivial additional difficulties, mostly owing to the broad distribution of the incoming neutrino energies
- Accurate theoretical models of electron- nucleus scattering provide a satisfactory description of the experimental data.

Motivations

- Quantitative understanding of the nuclear response to neutrino interactions needed for the interpretation of neutrino oscillation signals

- The description of the neutrino-nucleus cross section involves non trivial additional difficulties, mostly owing to the broad distribution of the incoming neutrino energies

- Accurate theoretical models of electron- nucleus scattering provide a satisfactory description of the experimental data.

- Data: MiniBooNE Collaboration

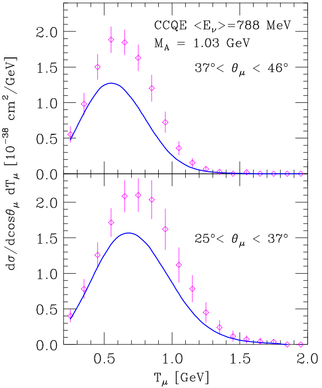

- Data: J.S. O'Connell *et al*

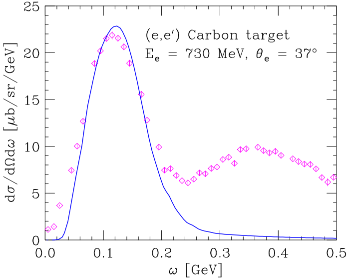

- The calculations performed using the spectral function and the measured nuclear vector form factors accurately reproduce the QE peak measured in electron scattering
- The same scheme largely fails to explain the MiniBooNE data.

QE neutrino-nucleus scattering

- The measured double differential CCQE cross section is averaged over the neutrino flux

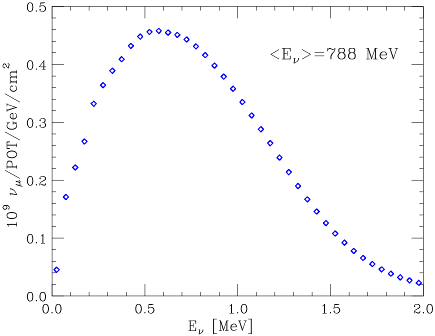

- Energy distribution of MiniBooNE neutrino flux
- Different reaction mechanisms contribute to the cross section at fixed θ_μ and T_μ.

A description of neutrino-nucleus interactions, has to be validated through extensive comparison to the large body of electron-nucleus scattering data.

The electron-nucleus x-section

- The double differential x-section of the process $e^- + A \to e^- + X$, can be written as

$$\frac{d^2\sigma}{d\Omega_{\mathbf{k}'} dk'_0} = \frac{\alpha^2}{Q^4} \frac{E'_e}{E_e} L_{\mu\nu} W_A^{\mu\nu} \ .$$

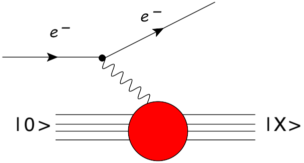

  - $L_{\mu\nu}$ is completely determined by the lepton kinematics
  - The hadronic tensor describes the response of the target nucleus.

$$W_A^{\mu\nu} = \sum_X \langle 0|J_A^{\mu\dagger}|X\rangle \langle X|J_A^\nu|0\rangle \, \delta^{(4)}(p_0 + q - p_X) \ ,$$

initial state

$|0\rangle$; p_0

final state

$|X\rangle = |1p; 1h\rangle, |2p; 2h\rangle \ldots$; p_X

Non relativistic nuclear many-body theory (NMBT) provides a fully consistent theoretical approach allowing for an accurate description of $|0\rangle$, independent on momentum transfer.

The *factorization "paradigm"*

- Simplest implementation: Impulse Approximation (IA)

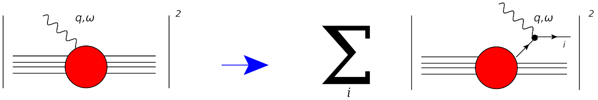

- At $|\mathbf{q}|^{-1} \ll d$:

$$J_A^\mu \longrightarrow \sum_i j_i^\mu \ , \qquad |X\rangle \longrightarrow |x, \mathbf{p}_x\rangle \otimes |R, \mathbf{p}_R\rangle \ ,$$

- The nuclear cross section can be traced back to the one describing the interaction with individual bound nucleons

$$d\sigma_A = \int dE d^3k \ d\sigma_N \ P(k, E)$$

  - An integration on the nucleon momentum and removal energy is carried out, with a weight given by the **Spectral Function**

Spectral function and energy-momentum distribution

- Oxygen spectral function, obtained within LDA.

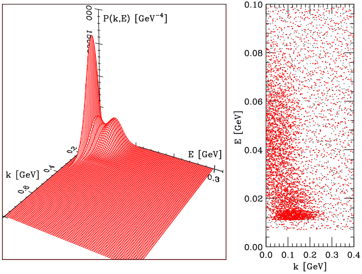

- Momentum and removal energy sampled from LDA (red) and RFGM (green) oxygen spectral functions

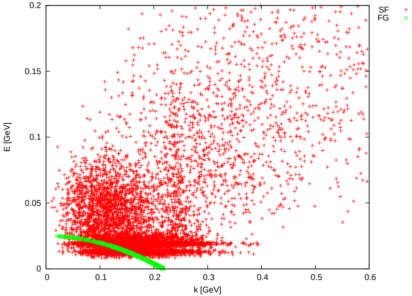

$$P_{LDA}(\mathbf{p}, E) = P_{MF}(\mathbf{p}, E) + P_{\rm corr}(\mathbf{p}, E)$$

$$\sum_{n \in \{F\}} Z_n |\phi_n(\mathbf{p})|^2 F_n(E - E_n) \qquad \int d^3r \varrho_A(\mathbf{r}) P^{NM}_{\rm corr}(\mathbf{p}, E; \varrho = \varrho_A(\mathbf{r}))$$

- Scattering off high momentum and high removal energy nucleons, providing ~ 20 % of the total strength.

Range of applicability of the IA

- Electron-Carbon cross section for $E_e = 1.3$ GeV, $\theta_e = 37.5$.

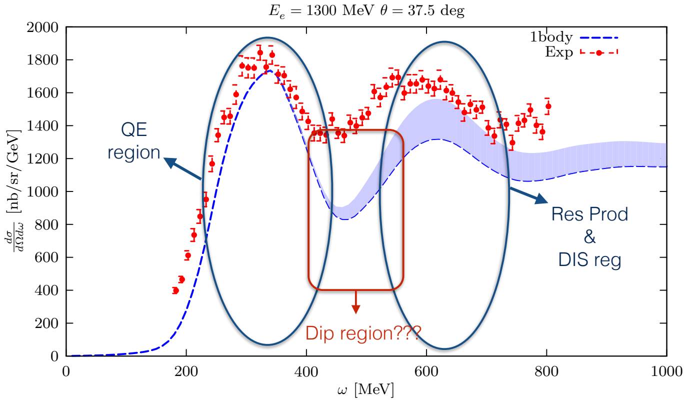

- The IA provides a unified framework, suitable to describe the measured cross section in different kinematical regimes, except in the *dip region*, where two-body currents are expected to contribute.

Role of reaction mechanism beyond IA

- Scaling functions associated with the longitudinal (L) and transverse (T) response of Carbon extracted from electron scattering data

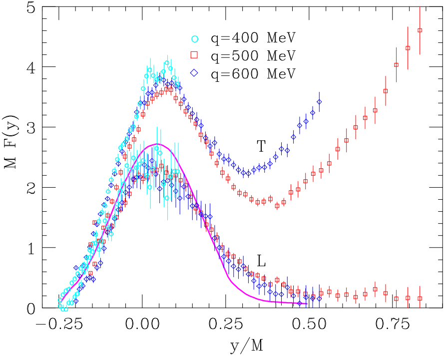

  - the onset of scaling is clearly visible in the region of QE peak, corresponding to $y \sim 0$.
  - large scaling violations appear in $F_T(y)$ at $y > 0$.

How can 2p2h final states be produced?

In a model accounting for NN correlations, 2p2h final states can be produced through 3 different reaction mechanisms.

- Initial State Correlations (ISC):

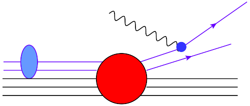

- Meson Exchange Currents (MEC):

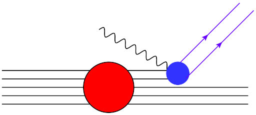

- Final State Interactions (FSI):

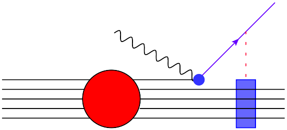

(a)

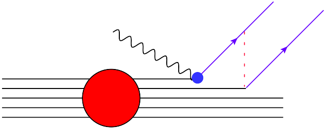

(b)

Extending the factorization scheme

- Using relativistic MEC and a realistic description of the nuclear ground state requires the extension of the factorization scheme to two-nucleon emission amplitude

  - Rewrite the hadronic final state $|X\rangle$ in the factorized form:

$$|X\rangle \longrightarrow |\mathbf{p}\ \mathbf{p}'\rangle \otimes |n_{(A-2)}\rangle = |n_{(A-2)}; \mathbf{p}\ \mathbf{p}'\rangle\ ,$$

    where $|n_{(A-2)}\rangle$ describes the spectator $(A-2)$-nucleon system, carrying momentum $\mathbf{p}_n$.

  - The two nucleon current simplifies

$$\langle X|{j_{ij}}^{\mu}|0\rangle \to \int d^3k d^3k' M_n(\mathbf{k},\mathbf{k}')\ \langle \mathbf{p}\mathbf{p}'|{j_{ij}}^{\mu}|\mathbf{k}\mathbf{k}'\rangle\ \delta(\mathbf{k}+\mathbf{k}'-\mathbf{p}_n)\ ,$$

  - The nuclear amplitude: $M_n(\mathbf{k},\mathbf{k}') = \langle n_{(A-2)}; \mathbf{k}\ \mathbf{k}'|0\rangle$
    is independent of **q**, and can therefore be obtained within NMBT.

Two nucleon spectral function

- Two-nucleon spectral function of uniform and isospin nuclear matter

$$P(\mathbf{k}, \mathbf{k}', E) = \sum_n |M_n(\mathbf{k}, \mathbf{k}')|^2 \delta(E + E_0 - E_n)$$

$$n(\mathbf{k}, \mathbf{k}') = \int dE \; P(\mathbf{k}, \mathbf{k}', E)$$

- Relative momentum distribution

$$n(\mathbf{Q}) = 4\pi |\mathbf{Q}|^2 \int d^3K \, n\left(\mathbf{Q} + \frac{\mathbf{K}}{2}, \mathbf{Q} - \frac{\mathbf{K}}{2}\right)$$

$$\mathbf{K} = \mathbf{k} + \mathbf{k}' \quad , \quad \mathbf{Q} = \frac{\mathbf{k} - \mathbf{k}'}{2} \; .$$

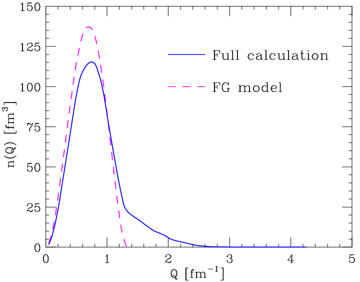

- Correlation effects lead to a quenching of the peak of the distributions and an enhancement of the high momentum tail

1p1h and 2p2h contributions to the nuclear cross section

- **The factorization scheme allows for a clear identification of the 1p1h and 2p2h contributions**

$$d\sigma = d\sigma_{\rm 1p1h} + d\sigma_{\rm 2p2h} \propto L_{\mu\nu}(W^{\mu\nu}_{\rm 1p1h} + W^{\mu\nu}_{\rm 2p2h})$$

- **2p2h response tensor**

$$W^{\mu\nu}_{2p2h} = \sum_{h,h'<k_F} \sum_{p,p'>k_F} \langle 0|J^{\mu\,\dagger}|\mathbf{hh'pp'}\rangle\langle\mathbf{hh'pp'}|J^\nu|0\rangle \times \delta(\omega + E_0 - E_{hh'pp'})\delta(\mathbf{q}+\mathbf{h}+\mathbf{h'}-\mathbf{p}-\mathbf{p'}) \ ,$$

- **Current operator in momentum space:**

$$J^\mu(\mathbf{k_1},\mathbf{k_2}) = j^\mu_1(\mathbf{k_1})\delta(\mathbf{k_2}) + j^\mu_2(\mathbf{k_2})\delta(\mathbf{k_1}) + j^\mu_{12}(\mathbf{k_1},\mathbf{k_2}) \ ,$$

$$W^{\mu\nu}_{2p2h} = W^{\mu\nu}_{2p2h,11} + W^{\mu\nu}_{2p2h,22} + W^{\mu\nu}_{2p2h,12}$$

Production of 2p2h final states

1. **Initial state correlations**
2. MEC, two-body response
3. Interference

Initial state correlations

Within the IA...

$$W^{\mu\nu}_{2p2h,11} = \int d^3k \int dE \; P_{2h1p}(\mathbf{k}, E) w^{\mu\nu}_{11}$$

$$P_{2h1p}(\mathbf{k}, E) = \sum_{h,h'<k_F} \sum_{p'>k_F} |\Phi^{hh'p'}_{k}|^2$$
$$\times \, \delta(E + e_h + e_{h'} - e_{p'}) \; ,$$

- appearence of the tail of the cross section, extending to large energy loss. This contribution amounts to $\sim$ 10% of the integrated spectrum.

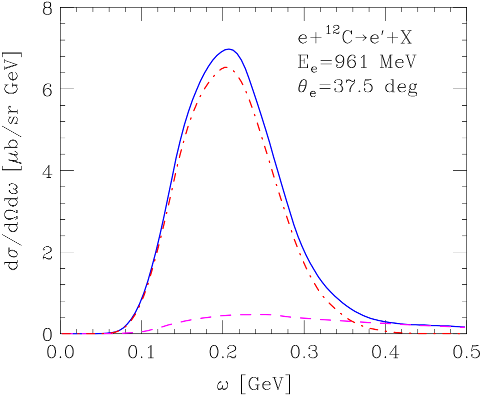

Production of 2p2h final states

1. Initial state correlations
2. **MEC, two-body response**
3. Interference

MEC: Pion exchange

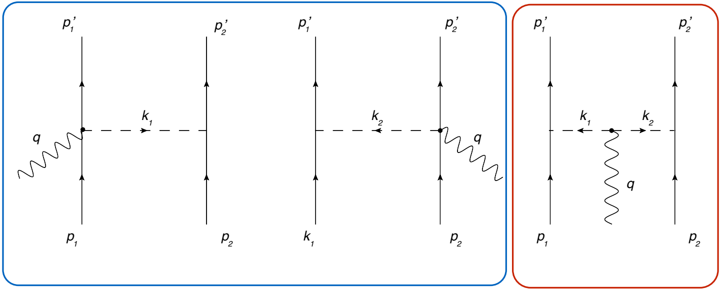

Seagull or contact term

Pion in flight term

MEC: Δ-isobar exchange

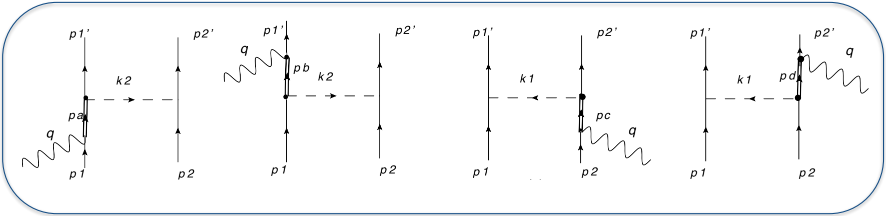

The Rarita-Schwinger (RS) expression for the Δ propagator reads

$$S^{\beta\gamma}(p, M_\Delta) = \frac{\not{p} + M_\Delta}{p^2 - M_\Delta^2}\left(g^{\beta\gamma} - \frac{\gamma^\beta\gamma^\gamma}{3} - \frac{2p^\beta p^\gamma}{3M_\Delta^2} - \frac{\gamma^\beta p^\gamma - \gamma^\gamma p^\beta}{3M_\Delta}\right)$$

WARNING

If the condition $p_\Delta^2 > (m_N + m_\pi)^2$ the real resonance mass has to be replaced by $M_\Delta \longrightarrow M_\Delta - i\Gamma(s)/2$ where $\Gamma(s) = \frac{(4f_{\pi N\Delta})^2}{12\pi m_\pi^2}\frac{k^3}{\sqrt{s}}(m_N + E_k)$.

2p-2h Transverse Response of nuclear matter

From the 2p-2h hadron tensor...

$$W^{\mu\nu}_{2p2h,22} = \int d^3k d^3k' d^3p d^3p' \int dE \; P_{2h}(\mathbf{k},\mathbf{k}',E) \langle \mathbf{k}\mathbf{k}'|j^{\mu}_{12}|\mathbf{p}\mathbf{p}'\rangle\langle \mathbf{p}\mathbf{p}'|j^{\nu}_{12}|\mathbf{k}\mathbf{k}'\rangle$$
$$\times \, \delta(\mathbf{k}+\mathbf{k}'+\mathbf{q}-\mathbf{p}-\mathbf{p}')\delta(\omega - E - e_p - e_{p'})\theta(|\mathbf{p}|-k_F)\theta(|\mathbf{p}'|-k_F) \; .$$

$$P_{2h}(\mathbf{k},\mathbf{k}',E) = \sum_{h,h'<k_F} |\Phi^{hh'}_{kk'}|^2 \delta(E + e_h + e_{h'})$$

- 12D integral, can be analitically reduced to a 7D integral $\rightarrow$ Monte Carlo integration technique
- both the direct and Pauli exchange contribution have to be considered (more than 100,000 terms) $\rightarrow$ Mathemathica and Fortran code

2p-2h Transverse Response of ^{12}C

Set of Harmonic Oscillator wave functions

$$\Psi_{0,0,0}(r) \Leftrightarrow \alpha = 1$$
$$\Psi_{0,1,1}(r) \Leftrightarrow \alpha = 2$$
$$\Psi_{0,1,-1}(r) \Leftrightarrow \alpha = 3$$

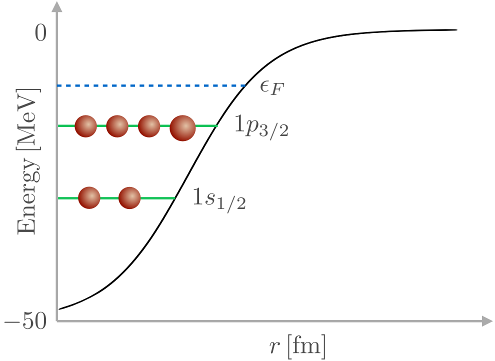

$$P_{2h}(\mathbf{k},\mathbf{k}',E) = \sum_{\alpha_1,\alpha_2=1}^{3} Z_{\alpha_1} Z_{\alpha_2} |\Psi_{\alpha_1}(k)|^2 |\Psi_{\alpha_2}(k')|^2 F(E + e_{\alpha_1}(k) + e_{\alpha_2}(k'))$$

$$e_1 = -38MeV \ , \ e_{2,3} = -17.0MeV \qquad Z_1 = 0.5 \ , \ Z_{2,3} = 0.625$$

Contribution of the MEC to the transverse response

Separate contributions to the transverse response function $R_T(\omega, q)$ at $q = 570$ MeV: pionic, pionic- Δ interference, Δ and total.

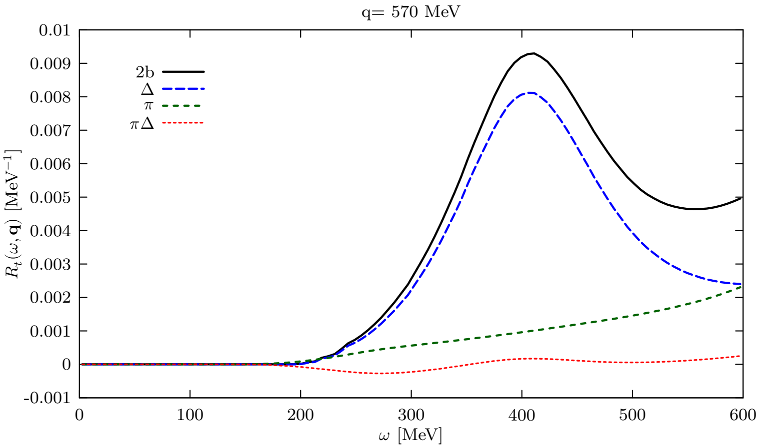

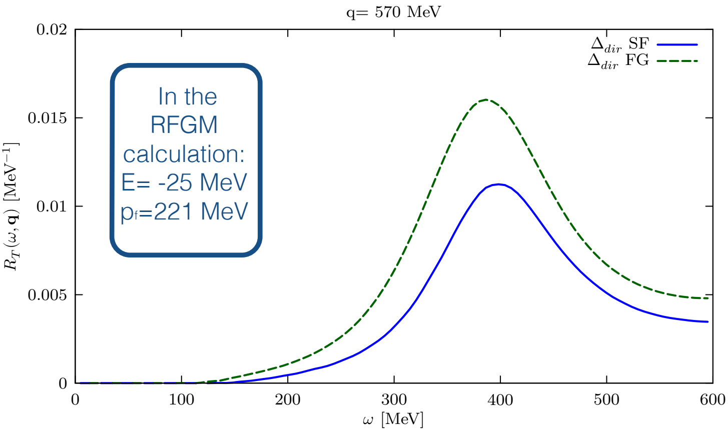

Sizable differences

Different threshold ⇒ different treatment of the initial state energies of the knocked-out nucleons.

Significant quenching of the response ⇒ short range correlations.

Production of 2p2h final states

1. Initial state correlations
2. MEC, two-body response
3. Interference

Interference term

It cannot be written in terms of SF…

$$W^{\mu\nu}{}_{2p2h,12} = \int d^3k\ d^3\xi\ d^3\xi'\ d^3h\ d^3h' d^3p\ d^3p' \phi^{hh'*}_{\xi\xi'} \Big[\Phi^{hh'p'}_{k} \langle \mathbf{k}|j^{\mu}_1|\mathbf{p}\rangle$$
$$+ \Phi^{hh'p}_{k} \langle \mathbf{k}|j^{\mu}_2|\mathbf{p}'\rangle\Big] \langle \mathbf{p},\mathbf{p}'|j^{\nu}_{12}|\boldsymbol{\xi},\boldsymbol{\xi}'\rangle \delta(\mathbf{h}+\mathbf{h}'+\mathbf{q}-\mathbf{p}-\mathbf{p}')$$
$$\times\,\delta(\omega + e_h + e_{h'} - e_p - e_{p'})\theta(|\mathbf{p}| - k_F)\theta(|\mathbf{p}'| - k_F) + \mathrm{h.c.}\ .$$

Additional difficulty… This term involves the product of nuclear amplitudes entering in $P(k, E)$ and $P(k, k', E)$

WARNING

This interference contribution would be zero if correlations were not accounted for!

^{12}C electromagnetic response

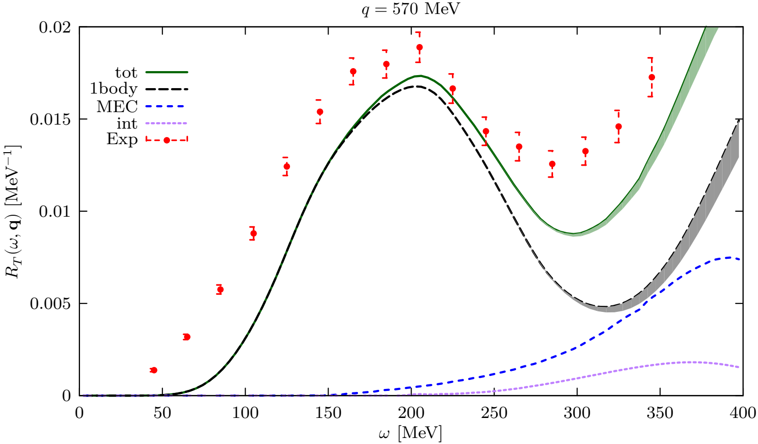

^{12}C calculations indicate a sizable enhancement of the electromagnetic transverse response.

Inclusion of Final State Interaction contribution

Convolution scheme

$$\frac{d\sigma^{\mathrm{FSI}}}{d\omega d\Omega} = \int d\omega' \; f_{\mathbf{q}}(\omega - \omega') \frac{d\sigma^{\mathrm{IA}}}{d\omega d\Omega}$$

The folding function can be decomposed in the form

$$f_{\mathbf{q}}(\omega) = \delta(\omega)\sqrt{T_A} + (1 - \sqrt{T_A})F_{\mathbf{q}}(\omega)$$

showing that the strength of FSI is driven by

- the nuclear transparency T_A
- the finite-width function $F_{\mathbf{q}}(\omega)$

- A.Ankowski *et al.*, Phys. Rev. D 91, 033005 (2015)
- O. Benhar, Phys. Rev. C 87, 024606 (2013).

e^- - ^{12}C inclusive cross section

The x-section can be rewritten in terms of R_T and R_L such as

$$\frac{d\sigma}{dE'_e d\Omega} = \sigma_{Mott}\left[\left(\frac{q^2}{\mathbf{q}^2}\right)^2 R_L + \left(\frac{-q^2}{2\mathbf{q}^2} + tan^2\frac{\theta}{2}\right) R_T\right]$$

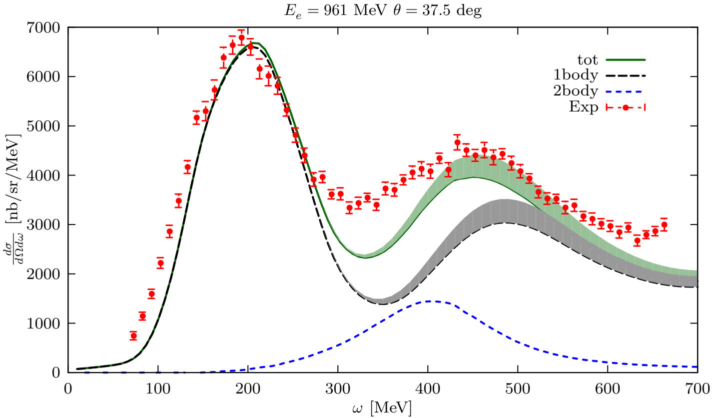

e^- - ^{12}C inclusive cross section

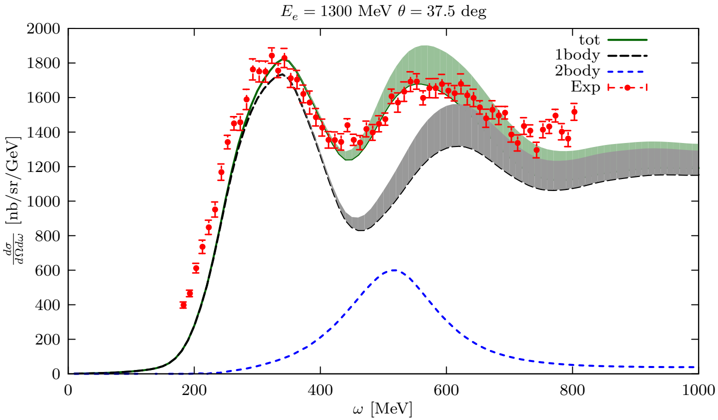

The contribution given by the interference term and MEC currents turns out to be sizable in the *dip* region.

e^{-} - ^{12}C inclusive cross section

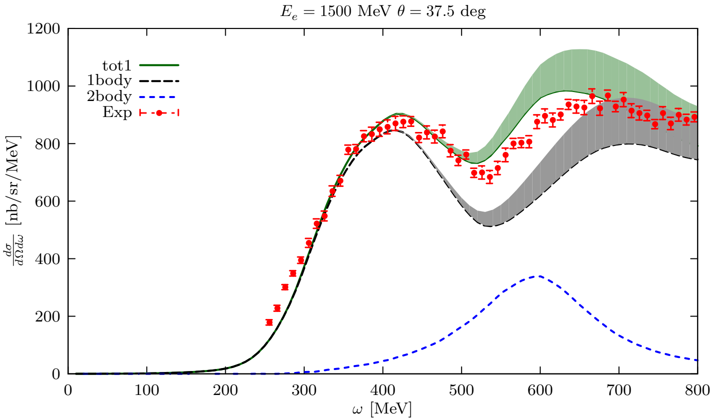

The contribution given by the interference term and MEC currents turns out to be sizable in the *dip* region.

Angular dependence of the two-body contribution

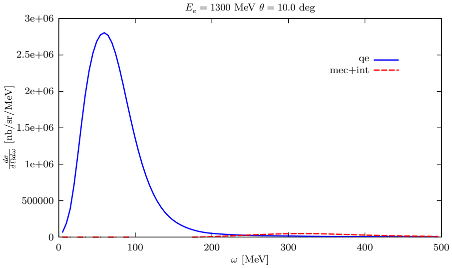

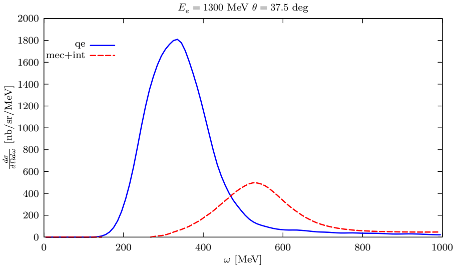

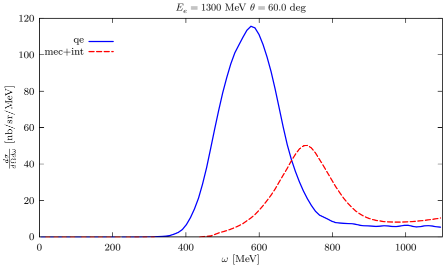

The relative strength due to two-body processes increases for larger values of the scattering angle where the transverse response becomes dominant .

Current & Future developments

- We are analysing the contribution of the interference between amplitudes involving the one- and two-body currents and 1p1h final states.
- We will implement our results in the determination of the nuclear response to electroweak probes. This requires the introduction of the one- and two-nucleon axial currents, and the calculation of the associated axial-axial and vector-axial responses for both the two-body and interference terms.
- We will apply our approach in the data analysis of new generation neutrino experiments which use liquid Argon detectors. To do that, it will be necessary to extend the spectral function formalism in order to describe the non-isospin symmetric nuclei.

backup slides

Inclusion of Final State Interaction contribution

- $f_{\mathbf{q}}(\omega - \omega' - U_V)$

- We consider $T_A = T_A(t_{kin})$ and $U_V = U_V(t_{kin})$ where

$$t_{kin} = \frac{E_k^2(1 - \cos\theta)}{M + E_K(1 - \cos\theta)}$$

- $F_{\mathbf{q}}(\omega)$ at $|\mathbf{q}| \sim 2$ GeV, including NN correlations

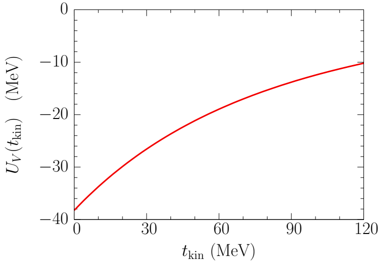

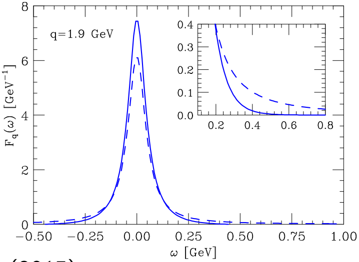

- A.Ankowski *et al.*, Phys. Rev. D 91, 033005 (2015)
- O. Benhar, Phys. Rev. C 87, 024606 (2013).

CCQE interactions at moderate ($|q| \lesssim 500$ MeV)

- Within NMBT the nucleus is described as a collection of A pointlike nucleons, the dynamics of which are described by the nonrelativistic Hamiltonian

$$H = \sum_{i=1}^{A} \frac{p_i^2}{2m} + \sum_{j>i=1}^{A} v_{ij} + \ldots$$

- Initial state definition:

$$H|0\rangle = E_0|0\rangle$$

- Final state definition

$$H|X\rangle = E_X|X\rangle$$

In the case of the MB experiment we will have that . . .

$$|X\rangle = |^{11}B, p\rangle \ , \ |^{11}C, n\rangle \ , |^{10}B, pn\rangle \ , |^{10}Be, pp\rangle \ldots$$

- The above Schrödinger equation can only be exactly solved for the ground- and low-lying excited states of nuclei with $A \leq 12$.

The nuclear current operator

- The nuclear Hamiltonian does not commute with the charge density operator: $[H, J^0] \neq 0$
- In order for the continuity equation to be satisfied two body currents are needed:

$$\frac{\partial}{\partial t} J^0 + \vec{\nabla} \cdot \vec{J} = 0$$

- The nuclear current includes one-and two-nucleon contributions

$$J^\mu_A(q) = \sum_{i=1}^{A} j_i^\mu(q) + \sum_{j>i=1}^{A} j_{ij}^\mu(q_1, q_2)\delta(q - q_1 - q_2)$$

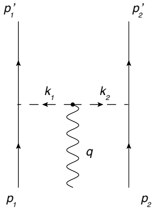

- non relativistic reduction of the current (q/m expansions) .

Kinematical range of accelerator-based neutrino experiments

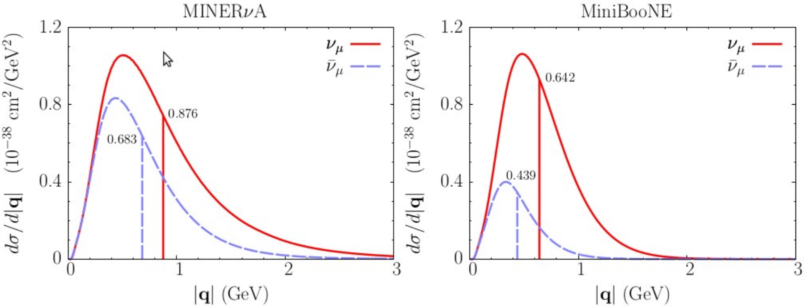

- $|q|$-dependence of CCQE cross section averaged with the Minerνa and MiniBooNE fluxes

WARNING!

unlike the ground state, the nuclear current operator and the nuclear final state depend on momentum transfer. At large **q** non relativistic approximations become inadequate.

The axial mass puzzle

- Unfolded total CCQE cross section

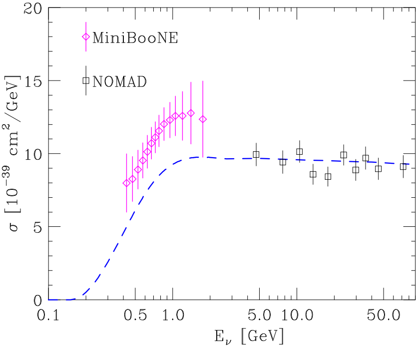

- ▸ The axial form factor is generally parametrized in the dipole form

$$F_A(Q^2) = \frac{g_A}{\left[1 + (Q^2/M_A^2)\right]^2} ,$$

- ▸ Deuteron data ⇒ $M_A \approx 1.03$ GeV
- ▸ MinibooNE ⇒ $M_A \approx 1.35$ GeV
- ▸ K2K ⇒ $M_A \approx 1.2$ GeV
- ▸ NOMAD ⇒ $M_A \approx 1.05$ GeV

- Interpret the value of M_A reported by MiniBooNE as an *effective* axial mass, modified by nuclear effects not included in the RFGM.
- The results of the calculations carried out using a realistic SF show that an even larger value of M_A is needed to fit the data.

Spectral function and energy-momentum distribution

- Oxygen spectral function, obtained within LDA.

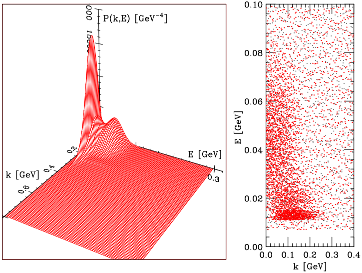

- Momentum and removal energy sampled from LDA (red) and RFGM (green) oxygen spectral functions

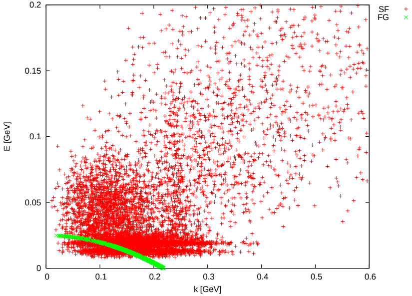

- FG model: $P_{RFGM}(p, E) \propto \theta(p_F - p)\ \delta(E_p - \epsilon + E)$,
- Scattering off high momentum and high removal energy nucleons, providing $\sim$ 20 % of the total strength, gives rise to 2p2h final states.

The impact of relativistic effects

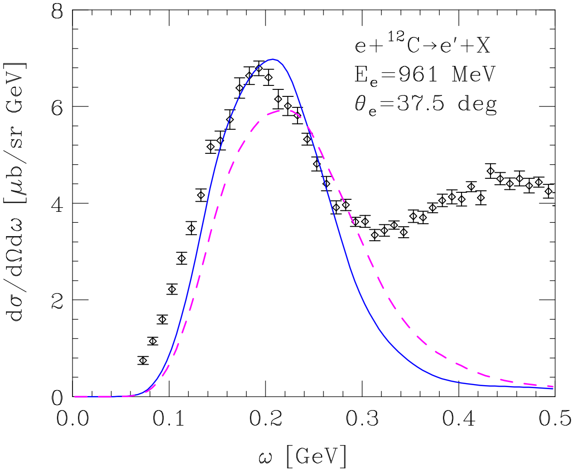

Electron-carbon cross section obtained within the IA approach using relativistic (solid line) and non relativistic (dashed line) kinematics.

- In a kinematical setup corresponding to $|q| \sim 585$ MeV at $\omega = \omega_{QE}$ relativistic kinematics sizeably affects both position and width of the quasi elastic peak.

Range of applicability of the IA

- Electron-Carbon cross section for $E_e = 1.3$ GeV, $\theta_e = 37.5$.

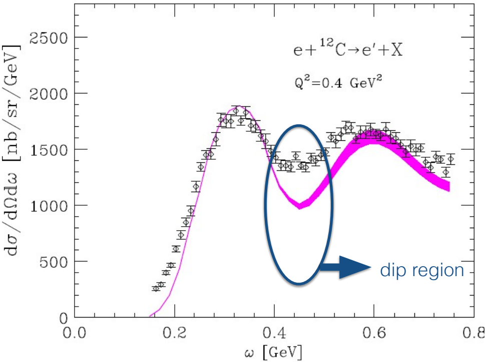

- The IA provides a unified framework, suitable to describe the measured cross section in different kinematical regimes, except in the *dip region*, where two-body currents are expected to contribute.

Different results obtained within GFMC and SF approach

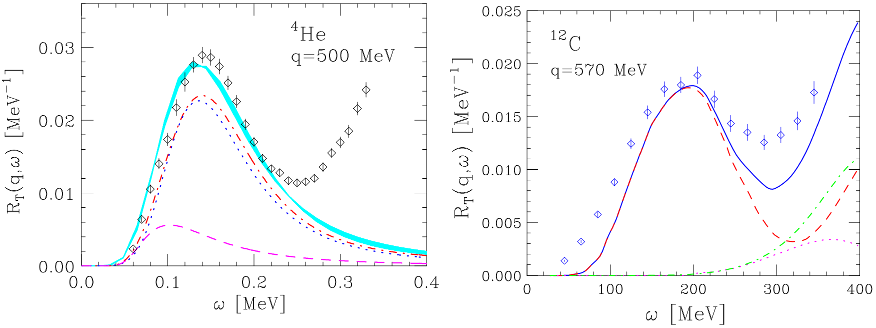

These differences should be ascribed to...

- Differences in the two-nucleon currents employed in the two cases
- The non relativistic nature of the GFMC calculations
- Interference between amplitudes involving the one- and two-body currents and 1p1h final states

May MEC explain the MiniBooNE data?

- It is apparent that the disagreement between theoretical calculations not including MEC and data is less pronounced at small θ_μ

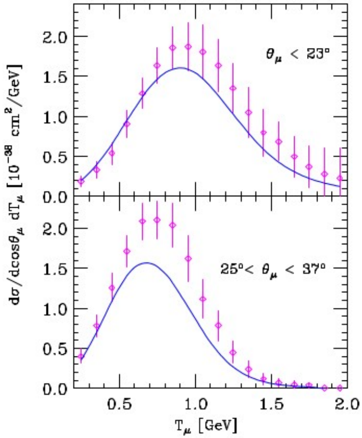

Non Relativistic expression of the 2p2h contribution to $R_T(\omega, q)$

PHYSICAL REVIEW C VOLUME 49, NUMBER 5 MAY 1994

Relativistic meson exchange and isobar currents in electron scattering: Noninteracting Fermi gas analysis

M. J. Dekker* and P. J. Brussaard
R. J. Van de Graaff Laboratory, University of Utrecht, P.O Box 80.000, 3508 TA Utrecht, The Netherlands

J. A. Tjon
Institute for Theoretical Physics, University of Utrecht, P.O Box 80.000, 3508 TA Utrecht, The Netherlands
(Received 22 November 1993)

$$\begin{aligned}\mathcal{R}_T = {}& 64c_N^2\left[2\frac{\mathbf{k}_1^2}{(\mathbf{k}_1^2+m_\pi^2)^2}+\mathbf{k}_{1_T}^2\left(2\frac{\mathbf{k}_1^2\mathbf{k}_2^2}{(\mathbf{k}_1^2+m_\pi^2)^2(\mathbf{k}_2^2+m_\pi^2)^2}-4\frac{\mathbf{k}_1^2}{(\mathbf{k}_1^2+m_\pi^2)^2(\mathbf{k}_2^2+m_\pi^2)}+\frac{1}{(\mathbf{k}_1^2+m_\pi^2)(\mathbf{k}_2^2+m_\pi^2)}\right)\right]\\ &+64c_\Delta^2\mathbf{k}_1^2\left(\mathbf{k}_1^2\mathbf{q}^2(2\tilde{b}^2+\tilde{a}^2)-(2\tilde{b}^2-\tilde{a}^2)(\mathbf{k}_1\cdot\mathbf{q})^2\right)\frac{1}{(\mathbf{k}_1^2+m_\pi^2)^2}+64c_\Delta^2\,\tilde{a}^2\,\frac{\mathbf{q}^4\mathbf{k}_{1_T}^2}{(\mathbf{k}_1^2+m_\pi^2)(\mathbf{k}_2^2+m_\pi^2)}\\ &+64c_\Delta c_N\,\tilde{a}\left(\frac{4\mathbf{q}^2\mathbf{k}_1^2\mathbf{k}_{1_T}^2}{(\mathbf{k}_1^2+m_\pi^2)^2(\mathbf{k}_2^2+m_\pi^2)}-2\frac{\mathbf{q}^2\mathbf{k}_{1_T}^2}{(\mathbf{k}_1^2+m_\pi^2)(\mathbf{k}_2^2+m_\pi^2)}-4\frac{\mathbf{k}_1^2\mathbf{k}_1\cdot\mathbf{q}}{(\mathbf{k}_1^2+m_\pi^2)^2}\right)+(1\leftrightarrow 2)\end{aligned} \quad (5.11)$$

The impact of relativistic effects in the two-body response

Relativity dramatically affects the behaviour of the response.

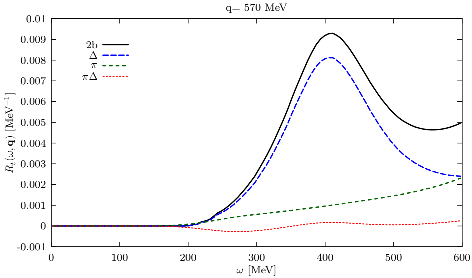

Relativistic

Nonrelativistic

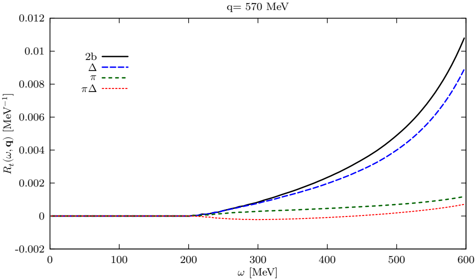

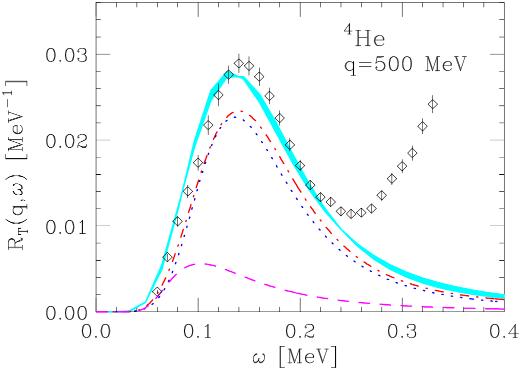

- Green's Function Monte Carlo calculation of the transverse electromagnetic response function of ^{4}He.
- MEC significantly enhance the transverse response function, not only in the dip region, but also in the quasielastic peak and threshold regions.

The relevance of the interference term. . . Sum Rule

- Sum rule of the electromagnetic response in the T channel

$$S_T(\mathbf{q}) = \int d\omega S_T(\mathbf{q},\omega), \quad S_T(\mathbf{q},\omega) = S^{xx}(\mathbf{q},\omega) + S^{yy}(\mathbf{q},\omega) \ ,$$

where

- $S^{\alpha\beta} = \sum_N \langle 0|J_A^\alpha|N\rangle\langle N|J_A^\beta|0\rangle\delta(E_0+\omega-E_N)$

- Need for a consistent treatment of *both* correlations and MEC currents.

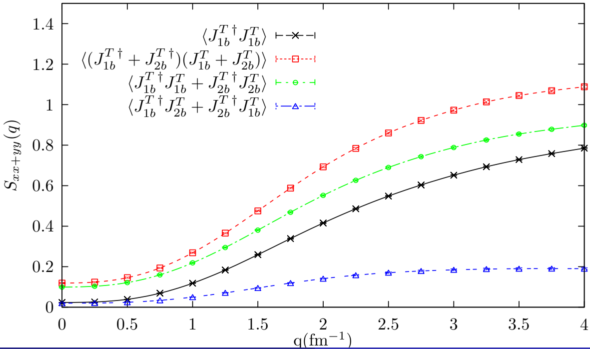

Contribution of different reaction mechanisms

- As neutrino beams are produced as secondary decay products their energy is broadly distributed
- The flux-averaged cross section at fixed $T\mu$ and θ_μ picks up contributions at different beam energies

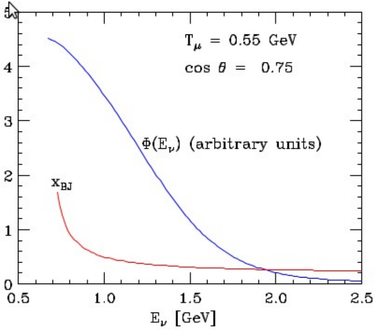

- x=0.5 $\to E_\nu = 0.788$ GeV , x=1 $\to E_\nu = 0.975$ GeV.
- $\Phi(0.975)/\Phi(0.788) = 0.83$

Two-body contribution within the SF anf FG formalism

The introduction of the two-nucleon current contributions in theoretical approaches based on the independent particle model (IPM) of nuclear structure, provides a quantitative wealth of the experimental data.

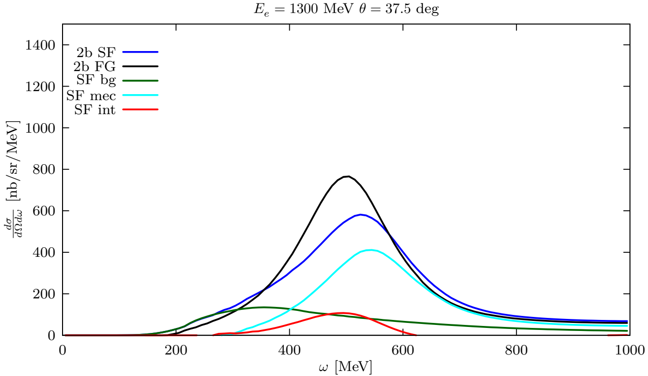

- The total two-body contribution obtained within the SF formalism do not differs too much from the FG result.

e^{-}-^{12}C cross section within the SF and FG formalism

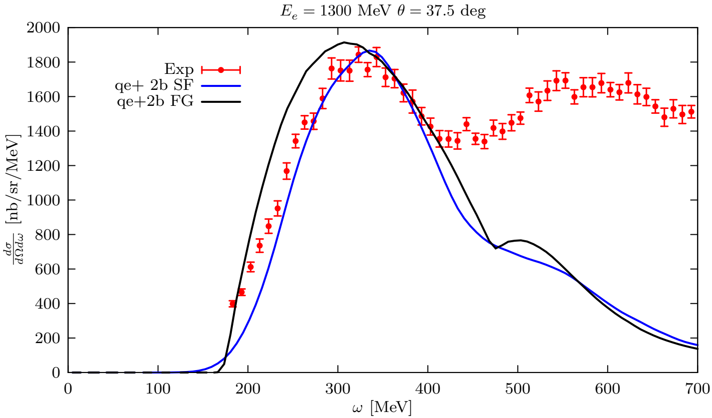

- While there are sizable differences both in the position and width of the QE peak, in the "dip" region the results obtained for the e^{-}-^{12}C cross section within the SF and FG approaches do no differ significantly.

"Flux averaged" QE electron-Carbon cross section

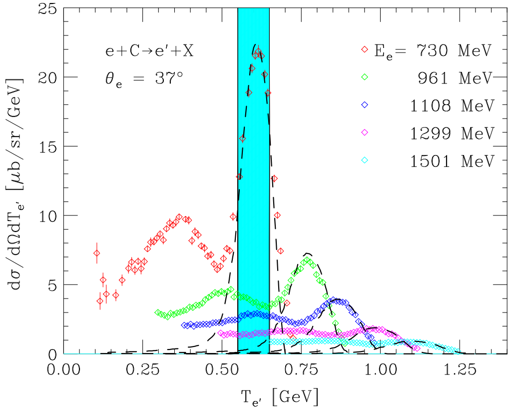

- Electron-Carbon scattering cross sections at $\theta_e = 37°$ plotted as a function of $T_{e'}$.
- Reaction mechanisms other that single-nucleon knockout contribute to the "flux-averaged" cross section.

- development of models based on a new paradigm, in which all relevant reaction mechanisms are *consistently* taken into account within a unified description of nuclear dynamics.

The IA x-section

- The hadronic tensor can be written in the simple form

$$W_A^{\mu\nu} = \int d^3p dE P(\mathbf{p}, E) \frac{M}{E_p} \left[Z W_p^{\mu\nu} + (A - Z) W_n^{\mu\nu} \right] ,$$

- Elements entering the definition of the IA x-section
  - the tensor describing the interactions of the i-th nucleon in free space

$$W_\alpha^{\mu\nu} = \sum_X \langle -\mathbf{p}_R, N | j^{\mu\dagger}_\alpha | X, \mathbf{p}_X \rangle \langle X, \mathbf{p}_X | j_\alpha^\nu | -\mathbf{p}_R, N \rangle \delta^{(4)}(\tilde{q} - p_R - p_X) .$$

$$\tilde{\omega} = E_X - \sqrt{\mathbf{p}^2 + M^2} = \omega + M - E - \sqrt{\mathbf{p}^2 + M^2}$$

  - The nucleon energy and momentum distribution, described by the hole spectral functions

Violation of current conservation

The replacement of ω with $\tilde{\omega}$ leads to a violation of the current conservation:

$$q_\mu w_N^{\mu\nu} = 0$$

Prescription proposed by *de Forest*:

$$\tilde{w}_N^{\mu\nu} = w_N^{\mu\nu}(\tilde{q})$$

$$\tilde{w}_N^{3\nu} = \frac{\omega}{|\mathbf{q}|} w_N^{0\nu}(\tilde{q})$$

The violation of gauge invariance only affects the longitudinal response. As a consequence, it is expected to become less and less important as the momentum transfer increases, electron scattering at large $|\mathbf{q}|$ being largely dominated by transverse contributions.

Local Density Approximation (LDA) P($\mathbf{k}, E$) for oxygen

$$P_{LDA}(\mathbf{p}, E) = P_{MF}(\mathbf{p}, E) + P_{\rm corr}(\mathbf{p}, E)$$

- $P_{MF}(\mathbf{p}, E) \rightarrow$ from $(e, e'p)$ data
- $P_{\rm corr}(\mathbf{p}, E) \rightarrow$ from uniform nuclear matter calculations at different densities:

$$P_{MF}(\mathbf{p}, E) = \sum_{n \in \{F\}} Z_n |\phi_n(\mathbf{p})|^2 F_n(E - E_n)$$

$$P_{\rm corr}(\mathbf{p}, E) = \int d^3 r \varrho_A(\mathbf{r}) P^{NM}_{\rm corr}(\mathbf{p}, E; \varrho = \varrho_A(\mathbf{r}))$$

Form factors

Hadronic monopole form factors

$$F_{\pi NN}(k^2) = \frac{\Lambda_\pi^2 - m_\pi^2}{\Lambda_\pi^2 - k^2}$$
$$F_{\pi N\Delta}(k^2) = \frac{\Lambda_{\pi N\Delta}^2}{\Lambda_{\pi N\Delta}^2 - k^2} \quad (1)$$

and the EM ones

$$F_{\gamma NN}(q^2) = \frac{1}{(1 - q^2/\Lambda_D^2)^2} \ ,$$
$$F_{\gamma N\Delta}(q^2) = F_{\gamma NN}(q^2)\left(1 - \frac{q^2}{\Lambda_2^2}\right)^{-1/2}\left(1 - \frac{q^2}{\Lambda_3^2}\right)^{-1/2} \quad (2)$$

where $\Lambda_\pi = 1300$ MeV, $\Lambda_{\pi N\Delta} = 1150$ MeV, $\Lambda_D^2 = 0.71 \mathrm{GeV}^2$, $\Lambda_2 = M + M_\Delta$ and $\Lambda_3^2 = 3.5 \ \mathrm{GeV}^2$.

Including MEC within the IPM

- J. Nieves *et al* , Phys. Lett. B **707**, 72 (2012)
- M. Martini *et al*, Phys. Rev.C **80**, 065501 (2009);

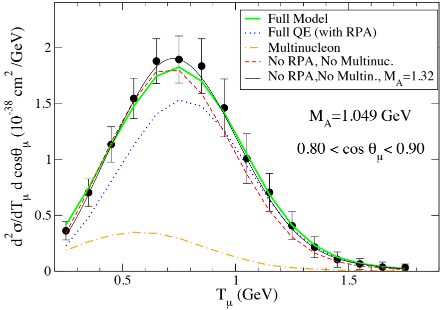

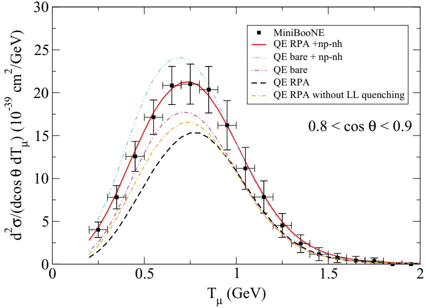

- After the inclusion of MEC, both schemes turn out to provide a quantitative account of the data
- A fully consistent treatment of 2p2h processes requires a realistic model of nuclear structure, taking into account the effects of NN correlations.

Neutral weak current two-body contributions

The enhancement due to two- nucleon currents, at $q \simeq 1\ \mathrm{fm}^{-1}$, is about 50% relative to the one-body values.

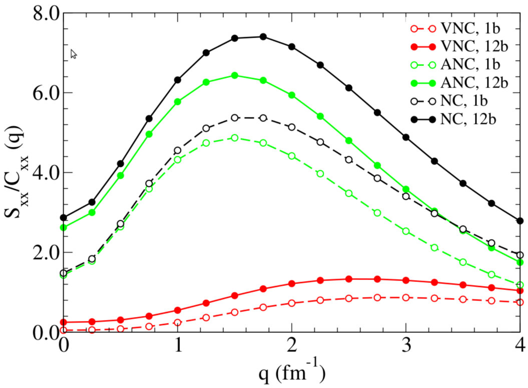

- Low momentum transfer the dominant contribution is given by: $\langle i | j_{2b}^\dagger j_{2b} | i \rangle$
- At higher momentum transfer: $\langle i | j_{2b}^\dagger j_{1b} | i \rangle + \langle i | j_{1b}^\dagger j_{2b} | i \rangle$ plays a more important role.

- A.Lovato *et al.*, Phys. Rev. Lett. 112, 182502 (2014)